Vasculogenic mimicry and breast cancer prognosis: Insights into predictive model development

ZHIFENG WU[1,2*], YUEYUE TENG[1*], SHENGCHAO HUANG[1,2], SHIMING SHI[1], PU QIU[1], LEYAO SHAN[1,2], MEIHUA LIN[1,2] and YUANQI ZHANG[1-3]

[1]Department of Breast Surgery, Affiliated Hospital of Guangdong Medical University, Zhanjiang, Guangdong 524000, P.R. China; [2]The First School of Clinical Medicine, Guangdong Medical University, Zhanjiang, Guangdong 524023, P.R. China; [3]Department of General Surgery, Guangdong Medical University Affiliated Hospital at XPCC Third Division, Tumxuk, Xinjiang Uygur Autonomous Region 843806, P.R. China

Received September 22, 2025; Accepted March 24, 2026

DOI: 10.3892/ol.2026.15600

Abstract. Breast cancer remains one of the most prevalent malignancies among women worldwide. Although advances in multimodal therapies have markedly improved clinical outcomes, recurrence and metastasis continue to pose major challenges. Vasculogenic mimicry (VM), a process in which tumor cells form vessel-like channels in the absence of endothelial cells, provides an alternative blood supply for tumor growth. The aim of the present study was to elucidate the association between VM and breast cancer prognosis and to establish a prognostic prediction model incorporating VM. The present study retrospectively analyzed 120 patients diagnosed with breast cancer and treated with curative surgery at Affiliated Hospital of Guangdong Medical University (Zhanjiang, China) between January 2020 and April 2022. Routine postoperative pathological assessment was performed, followed by CD34/periodic acid-Schiff double staining to detect VM structures within tumor tissues. Associations between VM and baseline characteristics, peripheral blood indices, pathological features and clinical variables were examined. Cox proportional hazards regression analysis was used to evaluate the prognostic significance of VM and a predictive model was constructed by integrating VM with other independent prognostic factors. Disease-free survival (DFS) was defined as the study endpoint. Model performance was evaluated and survival analysis was performed for individual risk factors as well as for the composite model. The presence of VM was reported to be significantly associated with advanced T stage (P=0.030), N stage (P=0.022), higher overall tumor stage (P=0.006) and elevated serum total cholesterol (P=0.015). VM positivity was associated with worse prognosis, with DFS significantly reduced in VM^+ patients (log-rank test; P<0.001). Multivariate analysis identified VM, N stage and Kiel-67 antigen (Ki-67) index as independent prognostic factors. A prediction model incorporating these variables demonstrated a robust performance, with a concordance index of 0.876 and a time-dependent area under the curve of 0.923, thereby providing strong support for individualized risk stratification and prognostic assessment in breast cancer. VM positivity, advanced nodal stage and a high Ki-67 index were reported to independently predict a reduced DFS following surgery. A prognostic model integrating VM, N stage and Ki-67 index exhibits high predictive accuracy and may serve as a valuable tool in evaluating the risk of recurrence and metastasis in the future.

Introduction

Breast cancer is the most common malignancy in women, accounting for ~30% of all new cancer cases among women (1). Epidemiological data indicated that since the early 2000s, its incidence has been increasing at an average annual rate of ~0.6%, posing a major global health challenge for women (1,2). Although advances in comprehensive treatment strategies have markedly improved patient survival, recurrence and metastasis remain notable obstacles in clinical management. Therapeutic decisions in breast cancer are typically guided by clinical stage, histological grade and hormone receptor status. However, breast cancer is inherently heterogeneous (3); thus, patients with identical staging and pathological features may experience markedly divergent outcomes despite receiving the same therapeutic regimen. The identification of reliable prognostic biomarkers is therefore key to enabling personalized and precise treatment.

Tumor angiogenesis is key to the growth, invasion and metastasis of malignancies. In addition to endothelial cell-driven angiogenesis, an alternative vascular-like structure originating directly from tumor cells has been identified in the tumor microenvironment, termed vasculogenic mimicry (VM).

Correspondence to: Professor Yuanqi Zhang, Department of Breast Surgery, Affiliated Hospital of Guangdong Medical University, 57 Renmin Avenue South, Zhanjiang, Guangdong 524000, P.R. China
E-mail: zhangyuanqi@gdmu.edu.cn

*Contributed equally

Key words: breast cancer, vasculogenic mimicry, disease-free survival, prognostic prediction model

First described by Maniotis *et al* (4) in uveal melanoma, VM is characterized by channels formed through the cooperation of tumor cells and extracellular matrix, mimicking the functional properties of blood vessels and providing nutrients through a non-endothelium-dependent mechanism. Subsequent studies have confirmed the presence of VM in an extensive spectrum of malignancies, including breast (5) and urological cancer (6), ovarian (7) and hepatocellular carcinoma (8).

VM not only contributes to neovascularization and sustains tumor growth but also serves a pivotal role in tumor cell migration during its formation (9). Therefore, VM is implicated not only in proliferation but also in metastatic dissemination. Multiple studies on breast cancer have demonstrated that VM is associated with unfavorable prognosis: Patients with VM^+ tumors tend to present with a large tumor size, advanced stage and short disease-free survival (DFS) and overall survival (5,10-12).

Further studies have revealed two principal aspects of the VM-breast cancer relationship. First, VM is strongly associated with clinicopathological characteristics. VM is positively associated with tumor size, lymph node metastasis and clinical stage (13), but negatively associated with hormone receptor expression, suggesting that VM^+ breast cancer cases often represent more aggressive subtypes. Of note, VM occurs at a markedly higher frequency in triple-negative breast cancer (TNBC) compared with that in non-TNBC cases (14). In addition, VM has been reported to be positively associated with human epidermal growth factor receptor 2 (HER2) upregulation (15), reinforcing its association with poor prognosis. Secondly, VM is closely associated with metastatic potential. Cancer stem cells (CSCs) serve a key role in tumor invasion and dissemination, and previous studies indicated that CSCs contribute to VM formation (14,16), suggesting that CSCs may promote metastasis through this mechanism. In a cohort of 331 surgically treated patients with breast cancer, Shirakawa *et al* (17) reported that VM^+ cases were more prone to hematogenous metastasis and exhibited markedly lower 5-year survival. Experimental models further demonstrated that VM is strongly associated with distant metastasis, particularly pulmonary spread (18).

Due to the central role of tumor vasculature in disease progression, anti-angiogenic therapies targeting endothelial cell-mediated angiogenesis have been developed to starve tumors of nutrients. However, these agents often exhibit limited efficacy or induce resistance. Previous research suggested that VM may increase following anti-angiogenic therapy and may represent a major mechanism of therapeutic resistance (5,19). Beyond anti-angiogenic agents, resistance to targeted therapies may also involve VM. For instance, $HER2^+$ breast cancer exhibits distinct aggressive clinical behavior. The introduction of HER2-targeted therapies has markedly improved patient outcomes; trastuzumab reduces recurrence by up to 40% within 10 years from surgery in early-stage breast cancer (20). In metastatic $HER2^+$ disease, combining trastuzumab with chemotherapy significantly prolongs the median time to disease progression from 4.6 to 7.4 months (21). Nevertheless, recurrence persists in 26% of early-stage $HER2^+$ patients within 10 years despite trastuzumab and >70% of metastatic $HER2^+$ tumors progress within 1 year under continuous therapy (20). VM has been implicated in this resistance, as trastuzumab-insensitive $HER2^+$ breast cancer cells have been reported to generate VM structures within angiogenic microenvironments (22).

Collectively, notable evidence supports a strong association between VM and adverse outcomes in breast cancer. Elucidating the relationship between VM and clinicopathological features, and integrating VM with other independent prognostic factors, may improve the accuracy of predictive models. Such models could refine postoperative risk stratification, enhance prognostic evaluation and ultimately inform individualized therapeutic strategies.

Based on this rationale, the present study hypothesized that VM was closely associated with an unfavorable prognosis in breast cancer. The present study systematically analyzed VM expression alongside clinicopathological parameters, explored its prognostic significance and constructed a predictive model combining VM with additional independent risk factors. The aim of the present study was to more accurately predict the risk of recurrence and metastasis following surgery, and to potentially provide a foundation for personalized treatment and clinical decision-making in the future.

Patients and methods

Clinical data

Study population. Patients who underwent surgery for breast cancer at the Department of Breast Surgery, Affiliated Hospital of Guangdong Medical University (Zhanjiang, China), between January 2020 and April 2022, and met the below inclusion criteria, were included in the present study. All patients had received standardized surgical treatment and postoperative paraffin-embedded pathological specimens were available. The mean age of the overall study cohort was 49.9±9.2 years (range, 31-73 years). The inclusion criteria were as follows: i) Female patients newly diagnosed with invasive breast carcinoma who underwent surgical resection; ii) complete clinical and follow-up data available; iii) no history of neoadjuvant chemotherapy, radiotherapy or endocrine therapy prior to surgery; iv) absence of other concurrent malignancies and no prior history of cancer; v) availability of intact paraffin-embedded pathological specimens suitable for histopathological analysis; and vi) receipt of standardized adjuvant therapy following surgery.

The exclusion criteria were as follows: i) History of other malignant tumors; ii) bilateral breast cancer or carcinoma *in situ*; iii) male breast cancer; iv) distant metastasis at diagnosis or lack of standardized adjuvant therapy; and v) poorly preserved postoperative specimens unsuitable for pathological assessment.

The histopathological analysis of breast cancer tissue sections, as well as the use of clinical data in the present study, were approved by the Ethics Committee of the Affiliated Hospital of Guangdong Medical University (approval no. PJKT2025-067; Zhanjiang, China).

Observational parameters. Clinical and pathological data, including age, body mass index (BMI), menstrual status (premenopausal or postmenopausal), tumor location (upper outer, lower outer, upper inner or lower inner quadrant), T stage (T1-T4), N stage (N0, N1-N2 or N3), overall tumor stage (I-III) (23), histological grade (G1-G3) (24), estrogen receptor (ER) status, progesterone receptor (PR) status,

Table I. Primary reagents used in the present study.

Reagent	Source	cat. no.	Dilution/concentration
CD34 antibody	Wuhan Servicebio Technology Co., Ltd.	GB11169	1:200
Horseradish peroxidase-conjugated goat anti-rabbit IgG	Wuhan Servicebio Technology Co., Ltd.	GB23303	1:200
Periodic acid-Schiff staining kit	Beyotime Institute of Biotechnology	C0142	Ready-to-use

CD34, cluster of differentiation 34; IgG, immunoglobulin G.

HER2 expression (negative or positive), Kiel-67 antigen (Ki-67) index, breast surgical approach (breast-conserving surgery or mastectomy) and axillary surgery type (sentinel lymph node biopsy or axillary lymph node dissection), were collected. Laboratory indices included carbohydrate antigen 15-3 (CA153), carcinoembryonic antigen (CEA), serum total cholesterol, triglycerides, uric acid, alkaline phosphatase, lactate dehydrogenase and albumin-to-globulin ratio.

Postoperative follow-up data were obtained through inpatient records, outpatient visits and telephone consultations. The primary endpoint was DFS, defined as the time from completion of surgery to the first occurrence of tumor recurrence, distant metastasis or mortality from any cause. For patients without events, follow-up was censored at the last contact, with the cut-off date set at March 2025. Local recurrence or metastasis was confirmed through enhanced computed tomography (CT), positron emission tomography-CT, biopsy or surgical pathology, bone scintigraphy or magnetic resonance imaging.

Methods

Primary reagents. The primary reagents used in the present study are summarized in Table I.

Immunohistochemical and histochemical double staining for VM. Breast cancer tissues were fixed in 10% neutral-buffered formalin at room temperature for 24-48 h, and then paraffin-embedded. Tissues were obtained from the Department of Pathology, Affiliated Hospital of Guangdong Medical University (Zhanjiang, China). Sections (5 μm thick) were prepared using a Leica 2155 rotary microtome (Leica Microsystems GmbH) and baked at 60˚C for 1 h prior to staining. VM was identified using CD34 immunohistochemistry combined with periodic acid-Schiff (PAS) histochemistry, according to the following procedure: i) Deparaffinization and rehydration: Sections were sequentially immersed in xylene I/II (10 min each), followed by a graded ethanol series (100, 95, 80 and 70%) and rinsed in distilled water; ii) antigen retrieval: Slides were heated to ~95-100˚C in citrate buffer (pH, 6.0) using a microwave oven (8 min at medium power, 8 min pause, then 7 min at medium-low power), cooled to room temperature and washed three times with PBS (pH, 7.4); iii) blocking of endogenous peroxidase: Sections were incubated in 3% hydrogen peroxide for 25 min at room temperature in the dark, followed by PBS washing; iv) serum blocking: Tissues were covered with 3% bovine serum albumin and incubated for 30 min at room temperature; v) primary antibody incubation: CD34 antibody (cat. no. GB11169; dilution 1:200; Wuhan Servicebio Technology Co., Ltd.) diluted in blocking buffer was applied and slides were incubated overnight at 4˚C in a humid chamber; vi) secondary antibody incubation: Following PBS washing, slides were incubated with HRP-conjugated goat anti-rabbit IgG (cat. no. GB23303; dilution 1:200; Wuhan Servicebio Technology Co., Ltd.) for 50 min at room temperature; vii) diaminobenzidine (DAB) chromogenic detection: Visualization was achieved with freshly prepared DAB solution. The reaction was monitored microscopically and terminated by rinsing with tap water. Positive staining appeared as brown deposits; viii) PAS staining: Following CD34 staining, slides were treated with periodic acid for 10 min, rinsed and incubated with Schiff's reagent for 30 min at 37˚C in the dark. Counterstaining was performed with hematoxylin for 30 sec at room temperature; and ix) mounting: Sections were dehydrated through a graded ethanol series, cleared in xylene and mounted with neutral balsam for evaluation under a light microscope.

The criteria to identify VM^+ and VM^- cases were pre-defined. For each case, five representative tumor fields were examined under a high magnification (x200) following CD34/PAS double staining. A VM^+ case was defined as the presence of PAS^+, $CD34^-$ patterned networks or vessel-like structures containing red blood cells, distinct from $CD34^+$ endothelial-lined vessels (4). To minimize subjective bias, two experienced pathologists independently assessed all sections in a blinded manner. Discordant cases were resolved by consensus review. Representative images of the stained sections were captured under light microscopy.

Statistical analysis. All analyses were conducted using R software (version 4.2.1; R Foundation for Statistical Computing; https://www.R-project.org/). All immunohistochemical staining experiments were independently repeated three times to ensure reproducibility. Patients were categorized into VM^+ and VM^- groups. Continuous variables were expressed as the mean ± SD if normally distributed or as median with interquartile range if non-normally distributed; categorical variables were reported as counts and percentages. Group comparisons were performed using an unpaired Student's t-test or Wilcoxon rank-sum test for continuous variables and χ^2 test or Fisher's exact test for categorical variables. $P<0.05$ was considered to indicate a statistically significant difference.

Univariate Cox proportional hazards regression was used to identify variables associated with DFS. Significant variables ($P<0.05$) were entered into a multivariate Cox regression model with forward stepwise selection used to determine independent

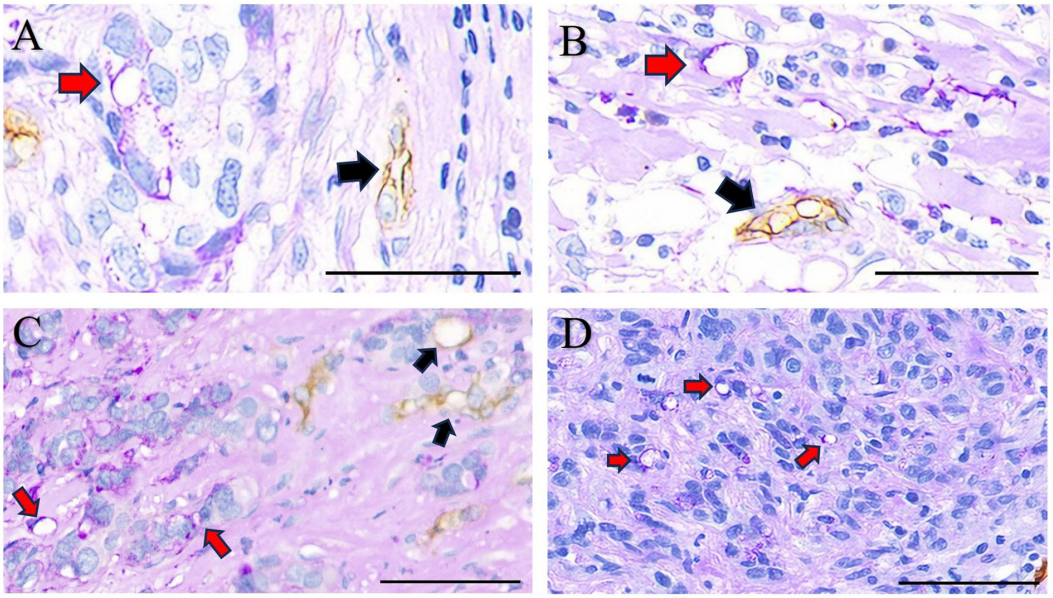

Figure 1. Pathological examination. All images were obtained using cluster of differentiation 34/periodic acid-Schiff immunohistochemical and histochemical double staining. VM is indicated by red arrows and normal blood vessels are indicated by black arrows. (A) Single VM channel with an adjacent normal blood vessel (magnification, x120). (B) Representative VM structure and adjacent endothelial-lined vessel (magnification, x110). (C) Multiple VM channels with normal blood vessels in the same field. (D) Clustered VM channels in tumor tissue (magnification, x75; scale bar, 50 μm). VM, vasculogenic mimicry.

prognostic factors. A nomogram was constructed based on the multivariate model using the 'rms' package (version 6.7-1; Frank E. Harrell Jr; https://CRAN.R-project.org/package=rms). The prognostic risk score was computed using the 'Predict()' function in R software, with the following formula: Risk score=exp (2.289 x VM + 1.491 x N stage + 0.057 x Ki-67 index). Internal validation was performed via bootstrap resampling, with a sample size of 40 per iteration and 800 repetitions. Model performance was assessed using the concordance index (C-index), time-dependent receiver operating characteristic (ROC) curves (using 'timeROC' package, version 0.4, Paul Blanche, https://CRAN.R-project.org/package=timeROC; and 'ggplot2' package, version 3.4.4, Hadley Wickham, https://CRAN.R-project.org/package=ggplot2) and calibration plots. Kaplan-Meier survival curves with log-rank tests were used to compare DFS between risk groups defined by independent prognostic factors and the composite risk score derived from the multivariate model (using 'survival' and 'survminer' packages, version 0.4.9, Alboukadel Kassambara, https://CRAN.R-project.org/package=survminer).

DFS was defined as the time from surgery to the first documented recurrence, metastasis or mortality from any cause. Patients without events were censored at the last follow-up date (March 2025).

Results

Histopathological findings. In accordance with the predefined inclusion and exclusion criteria, a total of 120 patients with breast cancer from between January 2020 and April 2022 with complete clinical records were retrospectively identified from the medical database of the Affiliated Hospital of Guangdong Medical University. All surgical specimens had been routinely formalin-fixed and paraffin-embedded in the Department of Pathology.

Dual CD34/PAS immunohistochemical and histochemical staining was performed on the paraffin sections. VM was detected in 29 cases, defined as PAS^+ and $CD34^-$ channels ($PAS^+/CD34^-$), whereas 91 cases were classified as VM^- ($PAS^+/CD34^+$) (Fig. 1).

Baseline characteristics and clinicopathological associates of VM. A total of 120 patients were included in the present study. Clinical information was extracted from initial surgical admission records. Laboratory indices, except for CA153 and CEA (measured within 1 week following standardized postoperative therapy) were obtained within 1 week prior to surgery. Pathological parameters were derived from postoperative histopathological assessments conducted in the Department of Pathology, Affiliated Hospital of Guangdong Medical University.

Of the 120 patients, 29 (24.17%) were VM^+ and 91 (75.83%) were VM^-. Patients were stratified into VM^+ and VM^- cohorts accordingly. The detailed demographic and clinicopathological characteristics of the cohort are summarized in Table II. Comparative analyses revealed significant intergroup differences in T, N and TNM stages and serum total cholesterol (all $P<0.05$), whereas no significant associations were observed for other variables. The median Ki-67 index among the entire study cohort (n=120) was 32% (interquartile range, 18-45%), while the median values for the VM- and VM+ subgroups were 30% (20-50%) and 40% (20-50%), respectively.

Univariate Cox proportional hazards regression analysis of DFS in patients with breast cancer. All patients were followed for a period ranging from 7 to 61 months, with a median follow-up of 43 months. During this period, 10 patients experienced recurrence or metastasis, whereas 110 patients remained disease-free. DFS was defined as the dependent variable, while baseline characteristics, peripheral blood biomarkers, pathological and clinical features, as well as the presence of VM,

Table II. Comparison of the clinicopathological features of patients with breast cancer according to VM status.

Characteristics	Reference range	Total no. of patients	VM^-	VM^+	P-value
Patients	-	120 (100)	91 (75.8)	29 (24.2)	-
Age, years	-	120	49.0±9.32	52.76±8.52	0.056[a]
BMI, kg/m^2	-	120	23.27±3.40	23.82±2.95	0.436[a]
Menstrual status					0.113[b]
Premenopausal	-	69	56 (46.7)	13 (10.8)	
Postmenopausal	-	51	35 (29.2)	16 (13.3)	
Tumor location					0.667[c]
Upper outer quadrant	-	80	63 (52.5)	17 (14.2)	
Lower outer quadrant	-	12	9 (7.5)	3 (2.5)	
Upper inner quadrant	-	22	15 (12.5)	7 (5.8)	
Lower inner quadrant	-	6	4 (3.3)	2 (1.7)	
T stage					0.030[c,d]
T1	-	37	32 (26.7)	5 (4.2)	
T2	-	77	56 (46.6)	21 (17.5)	
T3	-	4	1 (0.8)	3 (2.5)	
T4	-	2	2 (1.7)	0 (0.0)	
N stage					0.022[b,d]
N0-N1	-	101	81 (67.5)	20 (16.7)	
N2-N3	-	19	10 (8.3)	9 (7.5)	
TNM stage					0.006[c,d]
Stage I	-	28	25 (20.8)	3 (2.5)	
Stage II	-	70	55 (45.8)	15 (12.5)	
Stage III	-	22	11 (9.2)	11 (9.2)	
Histological grade					0.055[b]
G1-G2	-	60	50 (41.7)	10 (8.3)	
G3	-	60	41 (34.2)	19 (15.8)	
ER, %	-	120	70 (0-90)	0 (0-90)	0.325[e]
PR, %	-	120	10 (0-70)	0 (0-60)	0.194[e]
HER2 expression					0.956[b]
Negative	-	75	57 (47.5)	18 (15.0)	
Positive	-	45	34 (28.3)	11 (9.2)	
Ki-67 index, %	-	120	30 (20-50)	40 (20-50)	0.513[e]
Type of breast surgery					0.580[b]
Breast-conserving surgery	-	65	48 (40.0)	17 (14.2)	
Mastectomy	-	55	43 (35.8)	12 (10.0)	
Type of axillary surgery					0.107[b]
Sentinel lymph node biopsy	-	57	47 (39.2)	10 (8.3)	
Axillary lymph node dissection	-	63	44 (36.7)	19 (15.8)	
CA153, U/ml	≤25.0	120	13.19 (8.63-18.91)	15.91 (11.31-19.62)	0.098[e]
CEA, U/ml	≤5.0	120	1.50 (0.94-2.29)	1.65 (0.98-2.74)	0.684[e]
Total cholesterol, mmol/l	3.1-5.7	120	5.33 (4.50-5.89)	5.99 (5.13-6.67)	0.015[e]
Triglycerides, mmol/l	0.4-2.0	120	1.09 (0.78-1.61)	1.24 (0.83-1.71)	0.552[e]
Uric acid, μmol/l	155.0-357.0	120	290.6 (247.2-357.1)	279.4 (219.0-325.9)	0.247[e]
Alkaline phosphatase, U/l	31.0-115.0	120	69.9 (58.2-85.8)	76.1 (61.9-99.7)	0.125[e]
Lactate dehydrogenase, U/l	109.0-245.0	120	177.9 (166.7-206.9)	179.8 (164.3-196.0)	0.949[e]
Albumin-to-globulin ratio	1.5-2.5	120	1.642 (1.487-1.786)	1.667 (1.525-1.766)	0.907[e]

[a]Unpaired Student's t-test, [b]χ^2 test, [c]Fisher's exact test, [d]P<0.05 and [e]Wilcoxon rank-sum test. Values are expressed as n (%) the mean ± standard deviation or median (interquartile range). VM, vasculogenic mimicry; BMI, body mass index; ER, estrogen receptor; PR, progesterone receptor; IQR, interquartile range; HER2, human epidermal growth factor receptor 2; CEA, carcinoembryonic antigen; CA153, carbohydrate antigen 15-3; Ki-67, Kiel-67 antigen.

Table III. Univariate Cox proportional hazards regression analysis of disease-free survival in patients with breast cancer.

Variable	No. of patients	HR (95% CI)	P-value
VM			
Negative	91	Reference	-
Positive	29	7.813 (2.016-30.270)	0.003
Age, years	120	1.008 (0.943-1.078)	0.809
BMI, kg/m^2	120	1.032 (0.858-1.242)	0.738
Menstrual status			
Premenopausal	69	Reference	-
Postmenopausal	51	3.359 (0.868-13.002)	0.079
Tumor location			
Upper outer quadrant	80	Reference	-
Lower outer quadrant	12	5.137 (1.149-22.963)	0.032
Upper inner quadrant	22	1.731 (0.316-9.473)	0.527
Lower inner quadrant	6	3.708 (0.414-33.200)	0.241
T stage			
T1	37	Reference	-
T2	77	2.058 (0.436-9.718)	0.362
T3	4	0.000 (0.000-Inf)	0.998
T4	2	0.000 (0.000-Inf)	0.999
N stage			
N0-N1	101	Reference	-
N2-N3	19	5.775 (1.670-19.969)	0.006
TNM stage			
I	28	Reference	-
II	70	1.658 (0.185-14.845)	0.651
III	22	7.002 (0.817-60.010)	0.076
Histological grade			
G1-G2	60	Reference	-
G3	60	10.482 (1.323-83.029)	0.026
ER	120	0.981 (0.963-0.999)	0.043
PR	120	0.978 (0.952-1.006)	0.117
HER2 expression			
Negative	75	Reference	-
Positive	45	0.716 (0.185-2.773)	0.628
Ki-67 index	120	1.046 (1.018-1.075)	0.001
Surgical approach			
Breast-conserving surgery	65	Reference	-
Mastectomy	55	0.585 (0.164-2.091)	0.410
Axillary surgery			
Sentinel lymph node biopsy	57	Reference	-
Axillary lymph node dissection	63	1.304 (0.367-4.629)	0.681
CA15-3, U/ml	120	0.986 (0.908-1.070)	0.731
CEA, U/ml	120	0.707 (0.377-1.326)	0.279
Total cholesterol, mmol/l	120	1.096 (0.640-1.878)	0.737
Triglycerides, mmol/l	120	0.716 (0.273-1.876)	0.496
Uric acid, μmol/l	120	0.998 (0.991-1.006)	0.687
Alkaline phosphatase, U/l	120	1.009 (0.982-1.036)	0.515
Lactate dehydrogenase, U/l	120	1.004 (0.992-1.016)	0.529
Albumin/globulin ratio	120	1.048 (0.122-8.971)	0.966

CEA, carcinoembryonic antigen; CA153, carbohydrate antigen 15-3; Ki-67, Kiel-67 antigen; VM, vasculogenic mimicry; BMI, body mass index; ER, estrogen receptor; PR, progesterone receptor; HR, hazard ratio; CI, confidence interval; HER2, human epidermal growth factor receptor 2.

Table IV. Multivariate Cox proportional hazards regression analysis of disease-free survival in patients with breast cancer (n=120).

Variables	HR (95% CI)	P-value
VM (positive vs. negative)	9.824 (2.079-46.413)	0.004
N stage (N2-N3 vs. N0-N1)	4.358 (1.136-16.722)	0.032
ER	1.008 (0.985-1.032)	0.479
Ki-67 index	1.059 (1.015-1.105)	0.008
Histological grade (G3 vs. G1-G2)	3.270 (0.309-34.577)	0.325

HR, hazard ratio; CI, confidence interval; VM, vasculogenic mimicry; ER, estrogen receptor; Ki-67, Kiel-67 antigen.

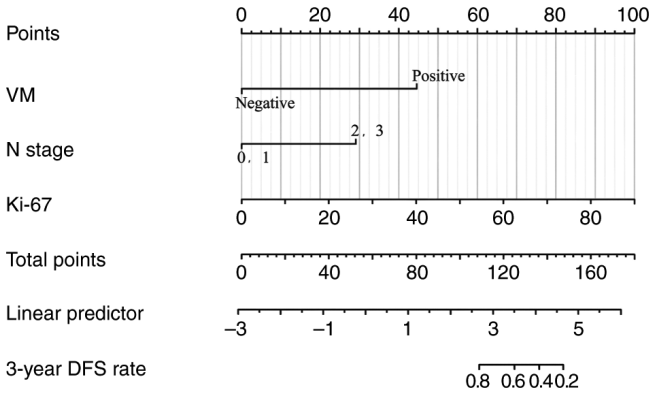

Figure 2. Nomogram of the prognostic prediction model for breast cancer. VM, vasculogenic mimicry; Ki-67, Kiel 67 antigen; DFS, disease-free survival.

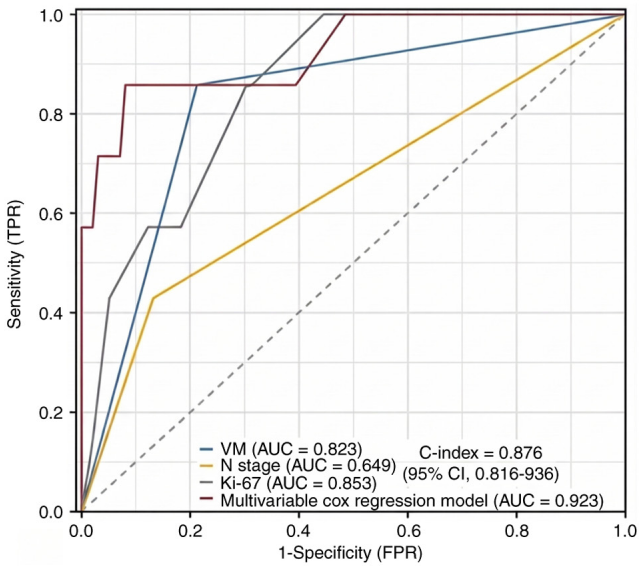

Figure 3. Time-dependent receiver operating characteristic curves for the multivariate Cox proportional hazards regression model predictions and independent risk factors. VM, vasculogenic mimicry; Ki-67, Kiel 67 antigen; AUC, area under the curve; TPR, true-positive rate; FPR, false-positive rate.

were included as independent variables in a univariate Cox proportional hazards regression model.

The analysis revealed that DFS was significantly associated with VM status [hazard ratio (HR)=7.813; 95% CI, 2.016-30.270; P=0.003], nodal stage (HR=5.775; 95% CI, 1.670-19.969; P=0.006), ER expression (HR=0.981; 95% CI, 0.963-0.999; P=0.043), Ki-67 index (HR=1.046; 95% CI, 1.018-1.075; P=0.001) and histological grade (HR=10.482; 95% CI, 1.323-83.029; P=0.026). Patients with a high Ki-67 index (≥30%) demonstrated a significantly shorter DFS compared with those with a lower Ki-67 index (P<0.001; Table III).

In combination, these findings indicated that VM, nodal stage, ER expression, Ki-67 index and histological grade are independent determinants of DFS in breast cancer. Among these, ER expression acted as a protective factor, whereas VM, advanced nodal stage, elevated Ki-67 index and higher histological grade were identified as adverse prognostic factors (Table III).

Multivariate Cox proportional hazards regression analysis of DFS in patients with breast cancer. As presented in Table IV, five variables with statistical significance in univariate analysis were included in the multivariate Cox regression model. The results demonstrated that VM (HR=9.824; 95% CI=2.079-46.413; P=0.004), N stage (HR=4.358; 95% CI=1.136-16.722; P=0.032) and Ki-67 index (HR=1.059; 95% CI=1.015-1.105; P=0.008) were identified as independent risk factors for DFS. By contrast, ER (P=0.479) and histological grade (P=0.325) were not statistically significant.

Construction and evaluation of the predictive model. Nomogram for the prognostic model. Based on the results of the multivariate Cox proportional hazards regression analysis, three independent prognostic risk factors, VM, N stage and the Ki-67 index, were ultimately incorporated into the predictive model.

In the present model, continuous variables were entered at their original values, while categorical variables were coded as follows: VM, negative=0 and positive=1; N stage, N0-N1=1 and N2-N3=2.

Subsequently, a prognostic nomogram was constructed to estimate the 3-year DFS of patients with breast cancer. Each covariate was assigned a point value by projecting upward to the corresponding scale. The individual scores of all variables were then summed to generate a total score, which was further mapped onto the probability scale at the bottom of the nomogram to yield the predicted 3-year DFS. A higher total score corresponded to a worse prognosis.

An investigation of the nomogram revealed that the Ki-67 index contributed the greatest weight to the model, followed by VM and N stage providing the smallest contribution (Fig. 2).

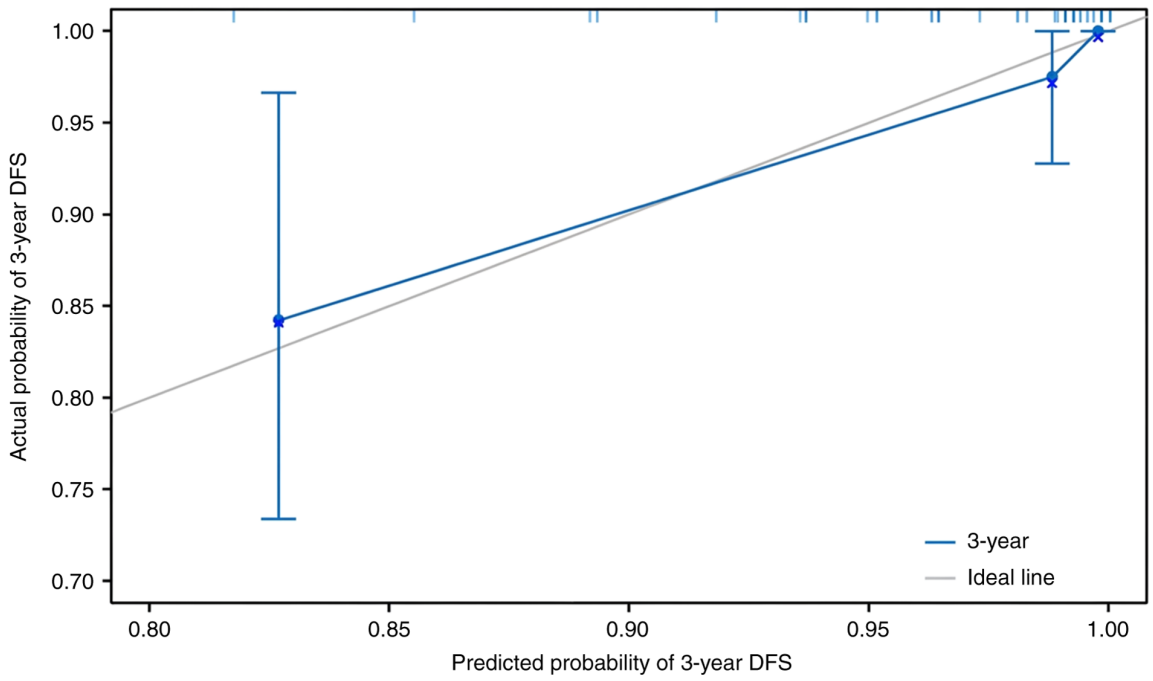

Figure 4. Calibration curve of the nomogram for predicting 3-year DFS in patients with breast cancer. X-axis denotes nomogram-predicted disease-free survival rate and y-axis denotes the actual DFS rate. DFS, disease-free survival.

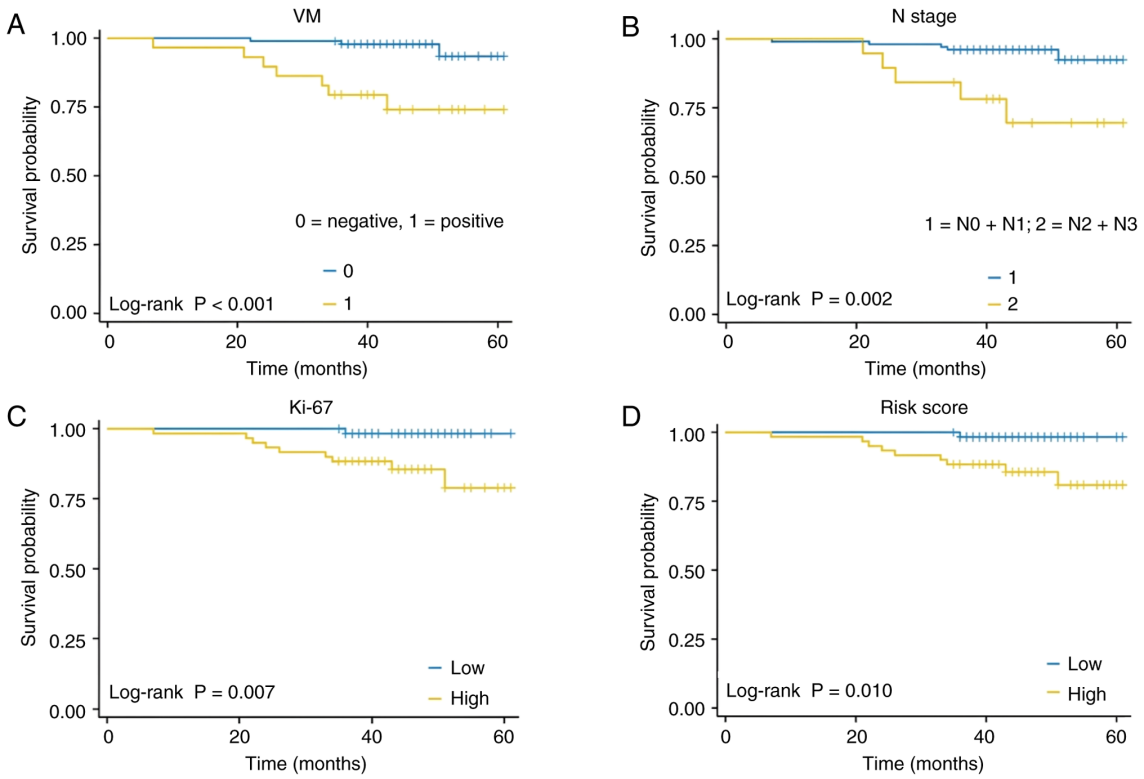

Figure 5. Kaplan-Meier survival analysis based on (A) VM status, (B) N stage, (C) Ki-67 index and (D) composite risk score derived from the multivariate Cox model. VM, vasculogenic mimicry; Ki-67, Kiel 67 antigen.

Evaluation of the predictive model. The predictive performance of the model was first assessed using the C-index computed in R software, yielding a value of 0.876 (95% CI, 0.816-0.936), indicative of notably enhanced discriminative ability. Subsequently, time-dependent ROC curve analysis was performed to compare the area under the curve (AUC) for individual risk factors and for the multivariate Cox proportional hazards model in predicting 3-year DFS. The results demonstrated that the AUCs were 0.823 for VM, 0.649 for N stage, 0.853 for the Ki-67 index and 0.923 for the multivariate

Cox regression model. As demonstrated in Fig. 3, the predictive accuracy of the multivariate model markedly outperformed that of any single factor, with a sensitivity of 85.7% and a specificity of 91.9% at the optimal cut-off value.

To further evaluate the prognostic reliability of the nomogram, calibration analysis was conducted using the 'rms' package in R software. Internal validation was performed via bootstrap resampling, with a sample size of 40 per iteration and 800 repetitions. As presented in Fig. 4, the calibration curve demonstrated close agreement between predicted and observed 3-year DFS probabilities, confirming the robust calibration and stability of the model.

Survival analysis. Survival analysis was performed for each independent prognostic factor, as well as for the integrated predictive model. Kaplan-Meier survival curves demonstrated that patients with VM^+ tumors exhibited significantly lower DFS compared with those patients with VM^- tumors (log-rank test; $P<0.001$). Similarly, patients with advanced N stage exhibited a significantly reduced DFS compared with those patients in the lower N stage group (log-rank test; $P=0.002$). A higher Ki-67 index (above the median) was also associated with a significantly worse DFS compared with a lower Ki-67 index (log-rank test; $P=0.007$). Furthermore, patients stratified into the high-risk group based on the risk score derived from the multivariate Cox regression model had a significantly worse DFS compared with those patients in the low-risk group (log-rank test; $P=0.010$). Although nodal stage and Ki-67 index were individually associated with DFS, the composite risk score demonstrated an improved discriminatory ability in stratifying patients. For example, patients with high risk scores exhibited a 3-year DFS of 58%, whereas those in the high N stage group alone had a 3-year DFS of 67% and those with high Ki-67 alone had a 3-year DFS of 62% (Fig. 5). These results suggested that the integrated risk score captures combined prognostic information beyond individual factors alone.

Collectively, these findings underscored that VM, N stage and the Ki-67 index represent independent prognostic determinants of postoperative DFS in breast cancer and that the risk score derived from the multivariate Cox proportional hazards model provides a robust tool in identifying patients at elevated risk of recurrence.

Discussion

Over recent decades, multiple studies have elucidated diverse risk factors associated with the prognosis of breast cancer (1,25). With the advent of increasingly sophisticated therapeutic strategies, the survival outcomes of patients have markedly improved (1,26). Nevertheless, disease recurrence and distant metastasis remain formidable clinical challenges, continuing to pose notable burdens for both patients and clinicians. While previous studies have examined the association between VM and poor prognosis in breast cancer (10,27,28), to the best of our knowledge, the present study was among the first to construct and internally validate a composite prognostic model that integrates VM status with established clinical parameters, including nodal stage and Ki-67 index. The development of a quantitative risk score enables more personalized risk stratification compared with analysis based solely on individual factors, offering a practical tool that may potentially guide postoperative decision-making in the future.

VM represents an alternative mechanism of tumor vascularization, in which tumor cells themselves form vascular-like channels independent of endothelial cells, thereby facilitating nutrient supply analogous to conventional vasculature. VM has been demonstrated to serve a key role in tumor growth, invasion and metastasis. Despite the intricate molecular pathways and signaling networks involved in its formation, both basic and clinical studies have consistently associated VM with adverse prognosis in patients with breast cancer (5,9,10,17). Of note, therapeutic interventions, particularly anti-angiogenic strategies, can inadvertently promote VM. By exacerbating hypoxic conditions within the tumor microenvironment, such treatments may stimulate VM formation and contribute to therapeutic resistance (29). Therefore, VM not only augments tumor aggressiveness but also undermines treatment efficacy, underscoring its potential value as a prognostic biomarker and a candidate variable in risk-prediction models for breast cancer.

In the present study, the presence of VM in invasive breast carcinoma was observed. A retrospective analysis of 120 patients with breast cancer was conducted in the present study and demonstrated that VM formation was reported to be associated with tumor stage, nodal involvement and overall disease stage. Specifically, the prevalence of VM positivity increased progressively with higher T and N classifications, as well as advancing clinical stage, corroborating its association with more aggressive disease phenotypes. Of note, no VM positivity was detected in T4 cases, likely attributable to limited sample size and the clinical tendency to prioritize neoadjuvant therapy over surgery in this subset. Furthermore, a significant association was identified between VM positivity and elevated serum cholesterol levels, a relationship that remains underexplored in the current literature (30-33). Since the phosphoinositide 3-kinase/protein kinase B (PI3K/AKT) signaling axis has been implicated in VM formation through the regulation of matrix metalloproteinase-9 and epithelial-mesenchymal transition (32), and that hypercholesterolemia has been reported to accelerate breast cancer progression through PI3K/AKT activation in murine models (33), it is plausible that elevated cholesterol may indirectly promote VM. This finding warrants further investigation with larger cohorts to substantiate the mechanistic association between dyslipidemia and VM formation in the future.

Hypercholesterolemia is often encountered in patients undergoing endocrine therapy and has been implicated in tumor progression through the modulation of cell membrane dynamics and signaling pathways (32,34,35). Whether dyslipidemia actively contributes to VM formation remains to be elucidated; however, these findings suggested that metabolic factors may be considered when interpreting postoperative tumor behavior. Routine assessment of lipid profiles may help identify patients at risk for aggressive features such as VM, warranting more comprehensive follow-up.

Consistent with previous studies (5,36), VM^+ patients in the present study cohort exhibited a trend toward higher histological

grade and reduced ER/PR expression, although these associations did not reach statistical significance, likely due to a limited sample size. Collectively, these findings strengthened the evidence that VM is a surrogate marker of tumor aggressiveness and an adverse prognostic determinant in breast cancer.

Univariate Cox regression analysis incorporating clinical, pathological and laboratory variables identified VM, nodal stage, Ki-67 index, ER status and histological grade as significant prognostic factors. Among these, VM, N stage and Ki-67 were confirmed as independent risk factors for reduced DFS in multivariate Cox regression models, whereas ER expression emerged as a protective factor. This finding aligns with existing literature highlighting these variables as prognostically relevant (37,38). Of note, tumor size (represented by T stage) and age, well-established predictors in meta-analyses of breast cancer prognostic models (39), did not reach statistical significance in the present study, likely reflecting the relatively small and demographically homogeneous cohort, as well as the biological heterogeneity of molecular subtypes that may confound conventional clinicopathological indicators.

Based on the multivariate Cox regression analysis, a prognostic model incorporating VM, N stage and Ki-67 index was constructed. This model demonstrated notably enhanced predictive performance, with a C-index of 0.876 and an AUC of 0.923, outperforming any individual factor. Calibration analysis confirmed a close agreement between predicted and observed outcomes, further supporting the robustness of the model. Kaplan-Meier analysis revealed a significantly worse DFS among VM^+ patients, patients with higher N stage and patients with elevated Ki-67 indices, in line with previous studies (40-42). Of note, the risk score derived from the present study model effectively stratified patients into high- and low-risk groups with distinct survival outcomes, thereby underscoring its clinical applicability.

Despite the established prognostic value of nodal metastasis and elevated Ki-67 index, the integrated risk score developed in the present study provided additional stratification by combining microanatomical features of tumor biology (namely, VM) with conventional clinical variables. By accounting for multiple determinants, this composite risk score may further identify patients at the highest risk of recurrence, potentially informing intensified surveillance or therapeutic strategies in the future.

It is key to recognize that the present study model currently lacks external validation and may be subject to overfitting due to internal training on a single cohort. Prospective validation in independent datasets is warranted to confirm predictive performance and generalizability.

In clinical practice, a high-risk classification may prompt consideration of more aggressive adjuvant therapy. While standardized guidelines for additional chemotherapy based on VM status are not yet established, patients with high composite risk scores could be candidates for multidisciplinary review, closer follow-up or enrollment in clinical trials evaluating adjuvant systemic treatments tailored by molecular and microarchitectural risk factors.

In conclusion, VM is significantly associated with adverse clinicopathological characteristics in breast cancer, including higher T and N stage, advanced tumor stage and elevated serum cholesterol levels. VM constitutes an independent adverse prognostic factor for breast cancer. N stage and Ki-67 index are independent predictors of recurrence and survival following surgery. A prognostic model integrating VM, N stage and Ki-67 index demonstrated high predictive accuracy and effectively stratified patients according to DFS risk.

Acknowledgements

Not applicable.

Funding

The present study was supported by the Jingyi Medical Research Foundation (grant no. JV112024-020122201).

Availability of data and materials

The data generated in the present study may be requested from the corresponding author.

Authors' contributions

ZW and YT contributed to the collection of clinical data, statistical analysis and drafting of the manuscript. SH and SS performed pathological evaluations and immunohistochemical analyses. PQ and LS assisted with database management and clinical interpretation. ML contributed to the analysis and interpretation of data, and critically revised the manuscript. YZ conceived and supervised the study and finalized the manuscript. All authors read and approved the final manuscript. ZW and YZ confirm the authenticity of all the raw data.

Ethics approval and consent to participate

The present study protocol was reviewed and approved by the Ethics Committee of the Affiliated Hospital of Guangdong Medical University (approval no. PJKT2025-067; Zhanjiang, China). Written informed consent was obtained from all participants prior to inclusion in the present study.

Patient consent for publication

Not applicable.

Competing interests

The authors declare that they have no competing interests.

References

1. Siegel RL, Giaquinto AN and Jemal A: Cancer statistics, 2024. CA Cancer J Clin 74: 12-49, 2024.
2. Han B, Zheng R, Zeng H, Wang S, Sun K, Chen R, Li L, Wei W and He J: Cancer incidence and mortality in China, 2022. J Natl Cancer Cent 4: 47-53, 2024.
3. Turner KM, Yeo SK, Holm TM, Shaughnessy E and Zhang X: Heterogeneity within molecular subtypes of breast cancer. Am J Physiol Cell Physiol 321: C343-C354, 2021.
4. Maniotis AJ, Folberg R, Hess A, Seftor EA, Gardner LM, Pe'er J, Trent JM, Meltzer PS and Hendrix MJ: Vascular channel formation by human melanoma cells in vivo and in vitro: Vasculogenic mimicry. Am J Pathol 155: 739-752, 1999.
5. Andonegui-Elguera MA, Alfaro-Mora Y, Cáceres-Gutiérrez R, Caro-Sánchez CHS, Herrera LA and Díaz-Chávez J: An overview of vasculogenic mimicry in breast cancer. Front Oncol 10: 220, 2020.

6. Lin X, Long S, Yan C, Zou X, Zhang G, Zou J and Wu G: Therapeutic potential of vasculogenic mimicry in urological tumors. Front Oncol 13: 1202656, 2023.
7. Tian X, Si Q, Liu M, Shi J, Zhao R, Xiong Y, Yu L, Cui H and Guan H: Advance in vasculogenic mimicry in ovarian cancer (review). Oncol Lett 26: 456, 2023.
8. Zheng N, Zhang S, Wu W, Zhang N and Wang J: Regulatory mechanisms and therapeutic targeting of vasculogenic mimicry in hepatocellular carcinoma. Pharmacol Res 166: 105507, 2021.
9. Andreucci E, Peppicelli S, Ruzzolini J, Bianchini F and Calorini L: Physicochemical aspects of the tumour microenvironment as drivers of vasculogenic mimicry. Cancer Metastasis Rev 41: 935-951, 2022.
10. Xing P, Dong H, Liu Q, Zhao T, Yao F, Xu Y, Chen B, Zheng X, Wu Y, Jin F and Li J: ALDH1 expression and vasculogenic mimicry are positively associated with poor prognosis in patients with breast cancer. Cell Physiol Biochem 49: 961-970, 2018.
11. Morales-Guadarrama G, García-Becerra R, Méndez-Pérez EA, García-Quiroz J, Avila E and Díaz L: Vasculogenic mimicry in breast cancer: Clinical relevance and drivers. Cells 10: 1758, 2021.
12. Pezzella F and Ribatti D: Vascular co-option and vasculogenic mimicry mediate resistance to antiangiogenic strategies. Cancer Rep (Hoboken) 5: e1318, 2022.
13. Shen R, Wu T, Huang P, Shao Q and Chen M: The clinicopathological significance of ubiquitin-conjugating enzyme E2C, leucine-rich repeated-containing G protein-coupled receptor, WW domain-containing oxidoreductase, and vasculogenic mimicry in invasive breast carcinoma. Medicine (Baltimore) 98: e15232, 2019.
14. Sun H, Yao N, Cheng S, Li L, Liu S, Yang Z, Shang G, Zhang D and Yao Z: Cancer stem-like cells directly participate in vasculogenic mimicry channels in triple-negative breast cancer. Cancer Biol Med 16: 299-311, 2019.
15. Liu T, Sun B, Zhao X, Gu Q, Dong X, Yao Z, Zhao N, Chi J, Liu N, Sun R and Ma Y: HER2/neu expression correlates with vasculogenic mimicry in invasive breast carcinoma. J Cell Mol Med 17: 116-122, 2013.
16. Liu TJ, Sun BC, Zhao XL, Zhao XM, Sun T, Gu Q, Yao Z, Dong XY, Zhao N and Liu N: CD133+ cells with cancer stem cell characteristics associates with vasculogenic mimicry in triple-negative breast cancer. Oncogene 32: 544-553, 2013.
17. Shirakawa K, Wakasugi H, Heike Y, Watanabe I, Yamada S, Saito K and Konishi F: Vasculogenic mimicry and pseudo-comedo formation in breast cancer. Int J Cancer 99: 821-828, 2002.
18. D'Andrea MR, Cereda V, Coppola L, Giordano G, Remo A and De Santis E: Propensity for early metastatic spread in breast cancer: Role of tumor vascularization features and tumor immune infiltrate. Cancers (Basel) 13: 5917, 2021.
19. Xu Y, Li Q, Li XY, Yang QY, Xu WW and Liu GL: Short-term anti-vascular endothelial growth factor treatment elicits vasculogenic mimicry formation of tumors to accelerate metastasis. J Exp Clin Cancer Res 31: 16, 2012.
20. Perez EA, Romond EH, Suman VJ, Jeong JH, Sledge G, Geyer CE Jr, Martino S, Rastogi P, Gralow J, Swain SM, *et al*: Trastuzumab plus adjuvant chemotherapy for human epidermal growth factor receptor 2-positive breast cancer: Planned joint analysis of overall survival from NSABP B-31 and NCCTG N9831. J Clin Oncol 32: 3744-3752, 2014.
21. Slamon DJ, Leyland-Jones B, Shak S, Fuchs H, Paton V, Bajamonde A, Fleming T, Eiermann W, Wolter J, Pegram M, *et al*: Use of chemotherapy plus a monoclonal antibody against HER2 for metastatic breast cancer that overexpresses HER2. N Engl J Med 344: 783-792, 2001.
22. Hori A, Shimoda M, Naoi Y, Kagara N, Tanei T, Miyake T, Shimazu K, Kim SJ and Noguchi S: Vasculogenic mimicry is associated with trastuzumab resistance of HER2-positive breast cancer. Breast Cancer Res 21: 88, 2019.
23. Amin MB, Edge SB, Greene FL, Byrd DR, Brookland RK, Washington MK, Gershenwald JE, Compton CC, Hess KR, Sullivan DC, *et al* (eds): AJCC cancer staging manual. 8th edition. Springer, New York, NY, pp 589-628, 2017.
24. Elston CW and Ellis IO: Pathological prognostic factors in breast cancer. I. The value of histological grade in breast cancer: Experience from a large study with long-term follow-up. Histopathology 19: 403-410, 1991.
25. Bray F, Laversanne M, Sung H, Ferlay J, Siegel RL, Soerjomataram I and Jemal A: Global cancer statistics 2022: GLOBOCAN estimates of incidence and mortality worldwide for 36 cancers in 185 countries. CA Cancer J Clin 74: 229-263, 2024.
26. Wagle NS, Nogueira L, Devasia TP, Mariotto AB, Yabroff KR, Islami F, Jemal A, Alteri R, Ganz PA and Siegel RL: Cancer treatment and survivorship statistics, 2025. CA Cancer J Clin 75: 308-340, 2025.
27. Wei Y, Jiao Z, Sun T, Lai Z and Wang X: Molecular mechanisms behind vascular mimicry as the target for improved breast cancer management. Int J Womens Health 15: 1027-1038, 2023.
28. Zheng S, Guo G, Yang Z, Lu Y, Lu K, Fu W and Huang Q: Vasculogenic mimicry regulates immune infiltration and mutational status of the tumor microenvironment in breast cancer to influence tumor prognosis. Environ Toxicol 39: 2948-2960, 2024.
29. Sun H, Zhang D, Yao Z, Lin X, Liu J, Gu Q, Dong X, Liu F, Wang Y, Yao N, *et al*: Anti-angiogenic treatment promotes triple-negative breast cancer invasion via vasculogenic mimicry. Cancer Biol Ther 18: 205-213, 2017.
30. Zipinotti Dos Santos D, de Souza JC, Pimenta TM, da Silva Martins B, Junior RSR, Butzene SMS, Tessarolo NG, Cilas PML Jr, Silva IV and Rangel LBA: The impact of lipid metabolism on breast cancer: A review about its role in tumorigenesis and immune escape. Cell Commun Signal 21: 161, 2023.
31. Gao W, Yao Y, Gao Q, Zhao T and Li H: Impact of serum lipids on prognosis in breast cancer patients: A systematic review and meta-analysis. World J Surg Oncol 23: 234, 2025.
32. Zhang X, Zhang J, Zhou H, Fan G and Li Q: Molecular mechanisms and anticancer therapeutic strategies in vasculogenic mimicry. J Cancer 10: 6327-6340, 2019.
33. Alikhani N, Ferguson RD, Novosyadlyy R, Gallagher EJ, Scheinman EJ, Yakar S and LeRoith D: Mammary tumor growth and pulmonary metastasis are enhanced in a hyperlipidemic mouse model. Oncogene 32: 961-967, 2013.
34. Li Y, Deng Z, Wang Y and Shen S: Lipid changes during endocrine therapy in early-stage breast cancer patients: A real-world study. Lipids Health Dis 23: 9, 2024.
35. Rillamas-Sun E, Kwan ML, Iribarren C, Cheng R, Neugebauer R, Rana JS, Nguyen-Huynh M, Shi Z, Laurent CA, Lee VS, *et al*: Development of cardiometabolic risk factors following endocrine therapy in women with breast cancer. Breast Cancer Res Treat 201: 117-126, 2023.
36. Shen Y, Quan J, Wang M, Li S, Yang J, Lv M, Chen Z, Zhang L, Zhao X and Yang J: Tumor vasculogenic mimicry formation as an unfavorable prognostic indicator in patients with breast cancer. Oncotarget 8: 56408-56416, 2017.
37. Zhu J, Cheng J, Ma Y, Wang Y, Zou Z, Wang W, Shi H and Meng Y: The value of inflammation-related indicators in chemotherapy efficacy and disease-free survival of triple-negative breast cancer. Eur J Med Res 30: 77, 2025.
38. Huang X, Luo Z, Liang W, Xie G, Lang X, Gou J, Liu C, Xu X and Fu D: Survival nomogram for young breast cancer patients based on the SEER database and an external validation cohort. Ann Surg Oncol 29: 5772-5781, 2022.
39. Phung MT, Tin Tin S and Elwood JM: Prognostic models for breast cancer: A systematic review. BMC Cancer 19: 230, 2019.
40. Mitra D, Bhattacharyya S, Alam N, Sen S, Mitra S, Mandal S, Vignesh S, Majumder B and Murmu N: Phosphorylation of EphA2 receptor and vasculogenic mimicry is an indicator of poor prognosis in invasive carcinoma of the breast. Breast Cancer Res Treat 179: 359-370, 2020.
41. Zhang Q, Peng S, Wang XM, Wang XX, Zhang HH and Liao LQ: Analysis of clinicopathologic characteristics and prognostic risk-factors in T1 stage breast cancer. Chin J Gen Surg 32: 761-770, 2023 (In Chinese).
42. Zhang ZW, Luo YB, Yang SH and Jiang BB: Association of Ki-67 expression with prognosis in patients with luminal B breast cancer. Matern Child Health Care China 39: 3140-3144, 2024 (In Chinese).